$$\Psi_{IM}{}^{(3b)}=\sum_{Ll}\sum_{\substack{K=\Omega\\(K>0,\Omega>0)}}(lLK0|lLIK)(\mathfrak{D}_{MK}{}^{I(+)*}\chi_{lK}{}^{(+)}\Phi_{L0}{}^{I}+\mathfrak{D}_{MK}{}^{I(-)*}\chi_{lK}{}^{(-)}\Phi_{L0}{}^{I}),$$

and

$$\Psi_{IM}{}^{(3c)}=\sum_{Ll}\Bigg(\sum_{\substack{K-\Omega>0\\(K>0,\Omega>0,K\neq\Omega)}}+\sum_{\substack{K-\Omega<0\\(K>0,\Omega>0,K\neq\Omega)}}\Bigg)$$

$$\times\Bigg\{\frac{1}{\sqrt{2}}(lL\Omega K-\Omega|lLIK)[\mathfrak{D}_{MK}{}^{I(+)*}(\chi_{l\Omega}{}^{(+)}\Phi_{L,K-\Omega}{}^{I(+)}+\chi_{l\Omega}{}^{(-)}\Phi_{L,K-\Omega}{}^{I(-)})$$

$$+\mathfrak{D}_{MK}{}^{I(-)*}(\chi_{l\Omega}{}^{(+)}\Phi_{L,K-\Omega}{}^{I(-)}+\chi_{l\Omega}{}^{(-)}\Phi_{L,K-\Omega}{}^{I(+)})]$$

$$+\frac{1}{\sqrt{2}}(lL\Omega K+\Omega|lLIK)[\mathfrak{D}_{MK}{}^{I(+)*}(\chi_{l\Omega}{}^{(+)}\Phi_{L,K+\Omega}{}^{I(+)}-\chi_{l\Omega}{}^{(-)}\Phi_{L,K+\Omega}{}^{I(-)})$$

$$+\mathfrak{D}_{MK}{}^{I(-)*}(\chi_{l\Omega}{}^{(+)}\Phi_{L,K+\Omega}{}^{I(-)}-\chi_{l\Omega}{}^{(-)}\Phi_{L,K+\Omega}{}^{I(+)})]\Bigg\}.$$

Corresponding to (2.8), we have

$$C_2{}^{x}\chi_{l\Omega}{}^{(\pm)}=\pm(-)^{-l}\chi_{l\Omega}{}^{(\pm)},\quad C_2{}^{y}\chi_{l\Omega}{}^{(\pm)}=\pm(-)^{-(l+\Omega)}\chi_{l\Omega}{}^{(+)},\quad\text{and}\quad C_2{}^{z}\chi_{l\Omega}{}^{(\pm)}=(-)^{-\Omega}\chi_{l\Omega}{}^{(\pm)},\tag{A3}$$

for $\Omega\neq0$.

PHYSICAL REVIEW VOLUME 129, NUMBER 5 1 MARCH 1963

Proton Scattering by Ni^{64} and Zn^{64} at 9.6 and 11.7 MeV*

J. BENVENISTE AND A. C. MITCHELL
Lawrence Radiation Laboratory, University of California, Livermore, California
AND
C. B. FULMER
Oak Ridge National Laboratory, Oak Ridge, Tennessee

(Received 13 July 1962; revised manuscript received 19 November 1962)

Differential cross sections for elastic scattering of protons from Ni^{64} and Zn^{64} were measured and compared. The observed shift in the positions of the maxima and minima of the differential cross sections is shown to be consistent with the presence of a symmetry energy term $[C(N-Z)/A]$ in the real nuclear potential of the optical model. It is found that $C\approx40$ MeV, in reasonable agreement with the results of other observations.

Comparison of the back-angle data yields an estimate of about 15 mb for the compound elastic-scattering cross section of Zn^{64} at 9.60 MeV. The 11.7-MeV data show no contribution from compound elastic scattering.

I. INTRODUCTION

ONE assumption adopted in the early development of the optical model[1,2] of the nucleus is that the depth of the real potential is independent of the mass number. This seemed quite reasonable in the beginning, in that any restrictions which could be placed on the many parameters used in fitting experimental data were welcome. This assumption has turned out to be quite fruitful. Remarkable success has been reported in describing the results of proton interactions with a wide range of nuclei over a large breadth of energies.

More recently, theoretical studies[3–22] have shown that there is reason to expect a difference between the proton-nucleus potential and the neutron-nucleus potential. The clearest contribution to this effect seems to be a

* Work performed under the auxpices of the U. S. Atomic Energy Commission.

[1] H. Feshback, C. E. Porter, and V. F. Weisskopf, Phys. Rev. **96**, 448 (1954).
[2] F. Bjorklund, S. Fernbach, and N. Sherman, Phys. Rev. **101**, 1832 (1956).
[3] M. H. Johnson and E. Teller, Phys. Rev. **98**, 783 (1955).
[4] A. E. S. Green and K. Lee, Phys. Rev. **99**, 772 (1955).
[5] A. E. S. Green, Phys. Rev. **99**, 1410 (1955).
[6] M. A. Melkanoff, S. A. Moszkowski, J. Nodvik, and D. S. Saxon, Phys. Rev. **101**, 507 (1956).
[7] L. Wilets, Phys. Rev. **101**, 1805 (1956).
[8] A. E. S. Green, Phys. Rev. **102**, 1325 (1956).
[9] A. A. Ross, H. Mark, and R. D. Lawson, Phys. Rev. **102**, 1613 (1956).
[10] A. A. Ross, R. D. Lawson, and H. Mark, Phys. Rev. **104**, 401 (1956).
[11] A. E. S. Green, Phys. Rev. **104**, 1617 (1956).
[12] H. A. Bethe, Physica **22**, 941 (1956).
[13] A. E. S. Green, K. Lee, and R. J. Berkley, Phys. Rev. **104**, 1625 (1956).
[14] A. M. Lane, Rev. Mod. Phys. **29**, 193 (1957).
[15] M. A. Melkanoff, J. Nodvik, and D. S. Saxon, Phys. Rev. **106**, 793 (1957).
[16] S. A. Moszkowski, in *Handbuch der Physik*, edited by S. Flügge (Springer-Verlag, Berlin, 1957), Vol. **39**, p. 411.
[17] S. Rand, Phys. Rev. **107**, 208 (1957).
[18] A. E. S. Green, and P. C. Sood, Phys. Rev. **111**, 1147 (1958).
[19] L. A. Sliv and B. A. Volchok, J. Exptl. Theoret. Phys. (U.S.S.R.) **36**, 539 (1959) [translation: Soviet Phys.—JETP **36(9)**, 374 (1959)].
[20] G. R. Satchler, Phys. Rev. **109**, 429 (1959).
[21] A. E. Glassgold and A. M. Lane, Compt. Rend. Congr. Intern. Phys. Nucl. Paris, 1958 (Dunod Cie, Paris, 1959), p. 23.
[22] A. M. Lane, Phys. Rev. Letters **8**, 171 (1962).

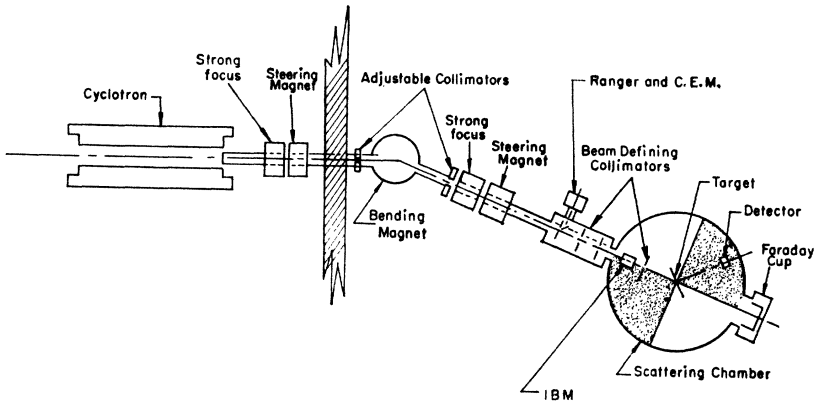

FIG. 1. Scattering geometry. The shaded sections of the scattering chamber indicate the regions in which observations were made.

combination of the Pauli exclusion principle and the spin-dependence of nuclear forces. These yield for the difference a linear dependence on the symmetry parameter

$$V_p - V_n = 2C(N-Z)/A,$$

with the constant, C, being variously given in the range 30 to 60 MeV.

Optical-model analyses of proton-nucleus elastic-scattering data[23–25] have shown that maxima and minima in elastic scattering angular distributions occur at angular positions that are determined mainly by VR^n, where R is the nuclear radius and n increases with proton energy. For the most part, previously reported proton elastic scattering data were obtained using target material with naturallly occurring isotopic abundances. Thus it may not be surprising that the above-mentioned detail of the proton-nucleus interaction escaped detection in the averaging effect of the several isotopes. On the other hand, careful measurements of elastic scattering from monoisotopic targets[26–33] have revealed differences which may be indicative of the presence of a symmetry energy term in the proton-nucleus potential. To pursue the experimental study of the symmetry energy term, we have tested the isobars Ni^{64} and Zn^{64}. Bombarding energies in the vicinity of 10 MeV were selected. At lower energies, compound elastic scattering is expected to obscure proper comparison[34,35] with optical-model predictions. At higher energies the influence of V on elastic-scattering angular distributions is smaller and observable effects due to the symmetry parameter seem to disappear.[36–38]

Measurements on these two isobars were previously performed at the Oak Ridge National Laboratory with 9.5-MeV protons. This energy was obtained with absorbers in the beam pipe to degrade the original 23-MeV beam from the cyclotron. Because of this, the observed energy resolution was about 10% and it was not possible to resolve the elastic from the inelastic group. This was especially troublesome at the back angles where the cross sections for the two groups were commensurable. Therefore, it was decided to repeat these observations with the variable-energy cyclotron of the Lawrence Radiation Laboratory at Livermore.

II. EXPERIMENTAL GEOMETRY

The geometry of the proton beam is shown in Fig. 1. Upon emerging from the cyclotron the beam is magnetically analyzed, focused, and collimated to a diameter of $\frac{1}{8}$ in. before it enters the scattering chamber. At the center of the scattering chamber is an eight-position target holder which is remotely controlled. On a rotatable table within the chamber are mounted radial tracks on which the detector may be quickly and accurately mounted. Table motion is remotely controlled and the table position readout, at a digital voltmeter in the control room, is precise to $\pm 0.1°$.

[23] A. E. Glassgold, W. B. Cheston, M. L. Stein, S. B. Sahuldt, and G. W. Erickson, Phys. Rev. **106**, 1207 (1957).
[24] A. E. Glassgold and P. J. Kellogg, Phys. Rev. **107**, 1372 (1957).
[25] J. S. Nodvik, in *Proceedings of the International Conference on the Nuclear Optical Model, Florida State University Studies*, No. 32 (The Florida State University Press, Tallahassee, Florida, 1959).
[26] R. Beurtey, P. Catillon, R. Chaminade, H. Faraggi, A. Papineau, and J. Thirion, Nucl. Phys. **13**, 397 (1959).
[27] R. A. Vanetsian, A. P. Klyucharev, and E. D. Fedchenko, At. Energ. (U.S.S.R.) **6**, 661 (1955).
[28] S. Kobayashi, K. Matsuda, Y. Nagahera, Y. Oda, and N. Yamanuro, J. Phys. Soc. Japan **15**, 1151 (1960).
[29] N. Y. Rutkevich, V. Ya. Golovnya, A. K. Val'ter and A. P. Klyucharev, Doklady Akad. Nauk, S.S.S.R. **130**, 1008 (1960) [translation: Soviet Phys.—Doklady **5**, 118 (1960)].
[30] A. P. Klyucharev and N. Ya. Rutkevich, J. Exptl. Theoret. Phys. (U.S.S.R.) **38**, 285 (1960) [translation: Soviet Phys.—JETP **11**, 207 (1960)].
[31] A. K. Val'ter, I. I. Zalyubovskii, A. P. Klyucharev, M. V. Pasechnik, N. N. Pucherov, and V. I. Chirko, J. Exptl. Theoret. Phys. **38**, 1419 (1960) [translation: Soviet Phys.—JETP **11**, 1025 (1960)].
[32] P. C. Gugelot, *Proceedings of the International Conference on Nuclear Structure, Kingston, Canada, 1960*, edited by D. A. Bromley and E. Vogt (University of Toronto Press, Toronto, 1960), p. 157.
[33] J. Benveniste, R. Booth, and A. C. Mitchell, Phys. Rev. **123**, 1818 (1961).
[34] W. F. Waldorf and N. Wall, Phys. Rev. **107**, 1602 (1957).
[35] C. A. Prescott and W. P. Alford, Phys. Rev. **115**, 389 (1959).
[36] M. K. Brussel and J. H. Williams, Phys. Rev. **114**, 525 (1959).
[37] R. A. Vanetsian, A. P. Klyucharev, and E. O. Fedchenko, At. Energ. (U.S.S.R.) **6**, 661 (1959).
[38] C. B. Fulmer, Phys. Rev. **125**, 631 (1962).

After traversing the scattering chamber, the unscattered beam is collected in a Faraday cup whose diameter is 3 in. A negatively biased grid placed just ahead of the cup suppresses the emergence of secondary electrons produced by the beam. The target foils were thicker than we customarily use; to assure ourselves, therefore, that none of the beam multiply scattered in the target was lost, an in-beam-monitor (ibm) was inserted in the scattering chamber just ahead of the target. The ibm consists of a small *p-n* junction diode which detects particles scattered at 150° from a thin (1.3 mg/cm²) aluminum foil suspended in the beam. The depletion layer is made thin enough so that the smallest pulses are made by the most energetic particles. Under these conditions, a discriminator may be set below these pulses to count virtually all the scattered particles. The count rate is found to be insensitive to the discriminator setting over an appreciable range. By comparing the ibm counts per unit charge (as measured with the Faraday cup) with the target in, then out, it was determined that no sensible beam was lost from the Faraday cup due to multiple scattering in the target. A multiple-scattering calculation confirmed that less than 0.1% of the beam would be scattered out of the acceptance angle of the Faraday cup. A similar amount would be lost by single scattering.

III. ENERGY MEASUREMENT AND CONTROL

Beside the entrance hole to the collimator, and separated from it by 0.030 in., is another hole. The beam entering this hole is scattered 90° through a variable absorber into a double proportional counter. An anticoincidence circuit permits us to make a differential range measurement of the incident beam with a precision of about 1%.

Back of the proportional counters is a CsI crystal and photomultiplier tube. After the range has been measured; only enough absorber is left in to allow about 1.5 MeV to be deposited in the crystal. Pulses from the photomultiplier tube are fed into a "continuous-energy monitor"—a circuit which measures the average height of input pulses and yields a continuously visible meter reading. Sensitivity checks show that throughout the course of our runs the incident energy was constant within ±0.15%.

IV. DETECTOR

The detector consists of a silicon *p-n* junction diode preceded by a gas proportional counter with offset center wire. Signals from the gas counter, proportional to dE/dx, and from the silicon crystal, proportional to the energy E, are fed into the two sides of a pulse multiplier network. The output from this network identifies the detected particle as a proton, deuteron, alpha particle, etc. This was used to gate the multichannel analyzer which recorded the proton spectra. Although this degree of sophistication was not necessary for a detector required to see elastically scattered protons, we found it useful for reducing background and for making clean observations of the inelastically scattered proton spectra. These latter observations will be described in another report.

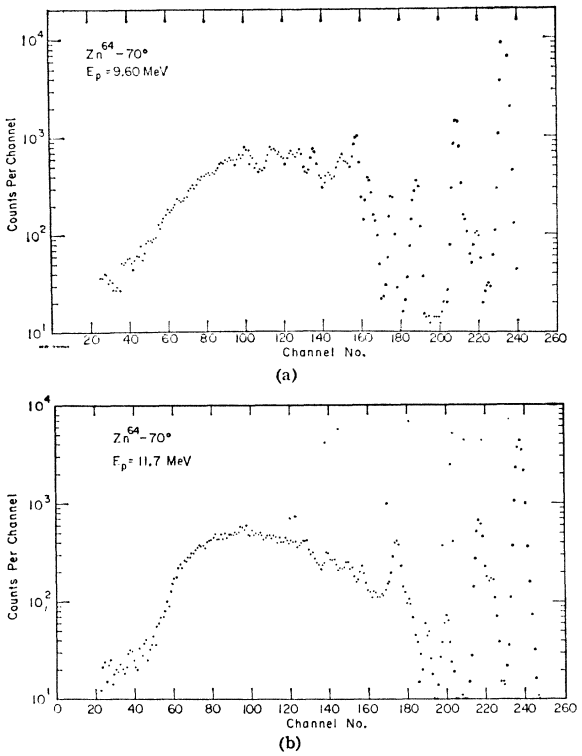

FIG. 2. Scattered spectrum. (a) E_p=9.6 MeV; (b) E_p=11.7 MeV.

V. TARGETS

Self-supporting foils of the two isobars were used as targets. The Ni^{64} target was prepared by E. B. Olzewski of the Isobars Division of the Oak Ridge National Laboratory. Ni^{64} was evaporated and deposited on a Ta backing which was lightly covered with Aquadag. The Ni^{64} foil was then peeled off the backing. The Zn^{64} foil was rolled from a bead of metal by F. Keresek of Argonne National Laboratory. The isotopic assay for each of the materials as given by the Isotopes Division of ORNL is given below:

Zn^{64} target:	Zn^{64}	Zn^{66}	Zn^{67}	Zn^{68}	Zn^{70}
	98.5%	1.1%	0.1%	0.3%	<0.1%
Ni^{64} target:	Ni^{58}	Ni^{60}	Ni^{61}	Ni^{62}	Ni^{64}
	1.99%	1.20%	0.14%	0.77%	95.9%

VI. EXPERIMENTAL PROCEDURE

These observations were performed with the aid of Scatterbrain, a control system which performs many of the necessary routine operations. This has been adequately described in earlier reports.[33,39]

[39] J. Benveniste, E. A. LaFranchi, G. E. Strahl, and R. L. Swenson, University of California Radiation Laboratory Report UCRL-5311, 1958 (unpublished).

TABLE I. Differential cross sections for elastic scattering of protons.

	E_p=9.60 MeV					
	Ni^{64}			Zn^{64}		
$\theta_{c.m.}$	$\sigma(\theta)$ (mb/sr)		σ/σ_R	$\sigma(\theta)$ (mb/sr)		σ/σ_R
20.3	10.0 ×10³	±6%	0.847	11.4 ×10³	±6%	0.877
25.4	4.22×10³	4.5	0.865	4.63×10³	4.5	0.828
30.5	2.27×10³	3.5	0.995	2.48×10³	3.5	0.918
35.5	1.42×10³	3.0	1.07	1.58×10³	3.0	1.05
40.6	805	3.0	1.02	927	3.0	1.03
50.7	230	3.5	0.679	307	3.5	0.791
60.8	62.3	3.0	0.359	91.8	3.0	0.461
65.8	38.5	3.0	0.297	55.5	3.0	0.373
70.9	31.5	3.0	0.316	38.6	3.0	0.336
75.8	33.1	3.0	0.418	34.2	3.0	0.373
80.9	36.5	3.0	0.567	36.4	3.0	0.494
90.9	38.5	3.0	0.873	40.5	3.0	0.800
95.9	35.8	3.0	0.964	38.2	3.0	0.893
100.9	31.4	3.0	0.982	35.7	3.0	0.973
110.9	19.7	3.0	0.798	25.7	3.0	0.909
120.8	10.1	3.0	0.507	15.2	3.0	0.668
125.8	6.63	4.0	0.368	10.9	4.0	0.526
130.7	4.64	3.0	0.278	7.68	3.0	0.403
135.6	4.02	4.0	0.262	5.76	4.0	0.326
140.6	4.33	4.0	0.300	5.53	4.0	0.334
150.5	7.50	3.0	0.576	8.14	3.0	0.545
160.3	11.4	3.0	0.945	12.9	3.0	0.936
170.2	15.5	3.0	1.35	17.8	3.0	1.35

Successive observations were customarily made in 20° steps. After two sweeps in which the angles were interleaved, data were available every 10° in the range from 20° to 170°. Further observations were made in those regions where better definition of the differential cross section was required. This procedure was expected to reveal any difficulties due to instrumental drifts. The two isobars were mounted in adjacent slots of the target changer and observations on the two were made successively at each angle setting. In addition, data from a Mylar target were obtained at each angle; these spectra were compared with those from Ni^{64} and Zn^{64} to obtain information about the carbon and oxygen impurities in the metallic foils. Typical spectra of scattered protons appear in Fig. 2.

The Ni^{64} foil was visibly nonuniform, so to have turned it in the customary way as the scattering angle was changed would have risked having the beam strike unpredictable amounts of scatterer. Therefore, the plane of the target changer was set so that it made an angle of 45° with the beam direction and then locked firmly in place. Under these conditions, the resolution, though not generally optimum, was still sufficiently good to resolve the elastic peak from the first level in all cases.

The nonuniformity of the Ni^{64} foil made a direct measurement of the average thickness traversed by the beam virtually impossible, so it was decided to normalize the cross section to that of another element. Originally the intent was to assume that at forward angles the cross section was essentially the Rutherford cross section, so that the thickness could be measured by comparing the scattered yield with that from a normal nickel foil. However, it was soon realized that if a symmetry energy were present the difference in this term for the major nickel isotopes and Ni^{64} would make this assumption invalid. Therefore, it was decided to normalize the ratio of the elastic-to-Rutherford cross section so that the peak in the vicinity of 40% rose to the same height as that peak for Zn^{64}. There is some reason for expecting this from the results of optical-model caluclations. It is expected that the Ni^{64} cross section relative to that measured for Zn^{64} is good to 5%. The normaliztaion procedure, of course, does not affect the magnitude of the observed shift.

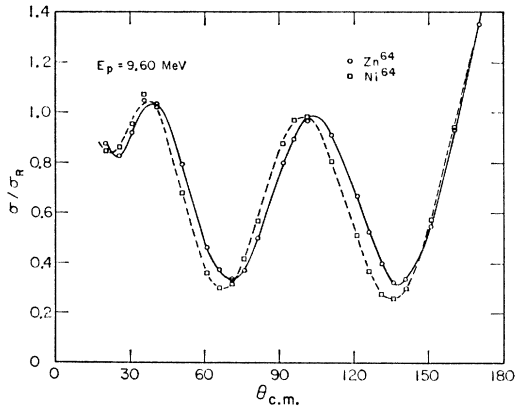

FIG. 3. Ratio to Rutherford cross section at 9.60 MeV.

VII. RESULTS AND CONCLUSIONS

Tables I and II contain the results of our elastic-scattering measurements. Corrections were made for the presence of impurities and for multiple scattering of the incident beam in the targets. The quoted errors

TABLE II. Differential cross sections for elastic scattering of protons.

	E_p=11.7 MeV					
	Ni^{64}			Zn^{64}		
$\theta_{c.m.}$	$\sigma(\theta)$ (mb/sr)		σ/σ_R	$\sigma(\theta)$ (mb/sr)		σ/σ_R
20.3	6.67×10³	±6%	0.836	8.26×10³	±6%	0.906
30.5	1.55×10³	4.5	0.973	1.64×10³	4.5	0.891
35.5				964	3.5	0.945
40.6	575	3.5	1.08	585	3.5	0.964
50.7	125	3.5	0.549	172	3.5	0.655
55.7	58.9	3.5	0.367	83.9	3.5	0.455
60.8	32.0	3.5	0.273	46.7	3.5	0.346
65.8	22.4	3.0	0.255	27.8	3.0	0.275
70.8	22.8	3.0	0.335	22.5	3.0	0.288
80.9	27.9	3.0	0.644	26.7	3.0	0.536
85.9				28.5	3.0	0.697
90.9	26.5	3.0	0.888	27.9	3.0	0.819
100.9	17.5	3.0	0.810	21.5	3.0	0.861
110.8	8.05	3.0	0.482	12.0	3.0	0.624
120.8	2.61	3.0	0.195	4.37	3.0	0.284
130.7	1.57	4.5	0.140	1.65	4.5	0.128
140.6	3.79	4.5	0.387	3.19	4.5	0.285
150.4	7.54	3.0	0.858	7.38	3.0	0.733
160.3	11.0	3.0	1.35	11.7	3.0	1.25
170.2	13.1	3.0	1.68	14.8	3.0	1.66

include contributions from statistics, beam current integrator measurements, uncertainty in the target angle setting, and target thickness measurement.

A puzzling feature of the original data[40] was that the absolute cross sections seemed to be 10–15% too large. We had learned to expect, from optical-model calculations and from experimental surveys,[27,38,41–43] smooth variations of elastic-scattering cross sections from element to element. Furthermore, previous experimental data[26,33] for nuclei in the region of Ni and Zn in the same energy region gave significantly lower values of the elastic cross section. In a search for the discrepancy a number of sources for systematic errors of this magnitude were considered. These included (1) an error of 1° in the measurement of scattering angle, (2) an error in the dead-time correction, (3) a 7° error in the target foil setting, (4) an error in the target thickness measurement, and (5) an error in the beam current measurement. The only one which survived subsequent tests was (3). A reasonable doubt remained as to whether the target angle was in error, because it was impossible to check this when it had become suspect.

A final check on the 9.60-MeV absolute cross sections was made almost a year later. For this measurement the detector, solid angle, target angle, etc., were different from those of the earlier run. To insure that sources of systematic errors had not been overlooked, elastic-scattering cross sections from Au were measured and found to agree within 1% with the Rutherford cross sections. Then differential cross sections for elastic scattering from Zn^{64} were remeasured at several angles. The agreement with the earlier data was, in each case, well within the quoted errors.

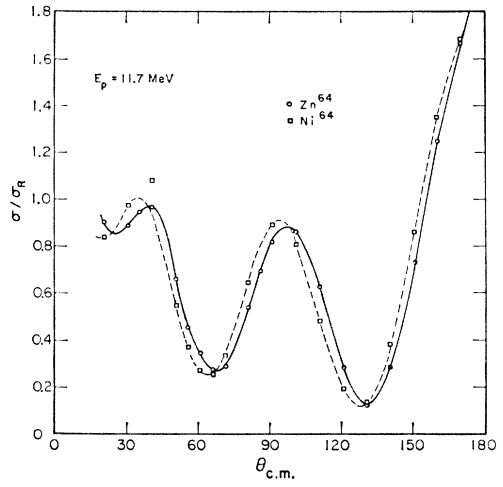

FIG. 4. Ratio to Rutherford cross section at 11.7 MeV.

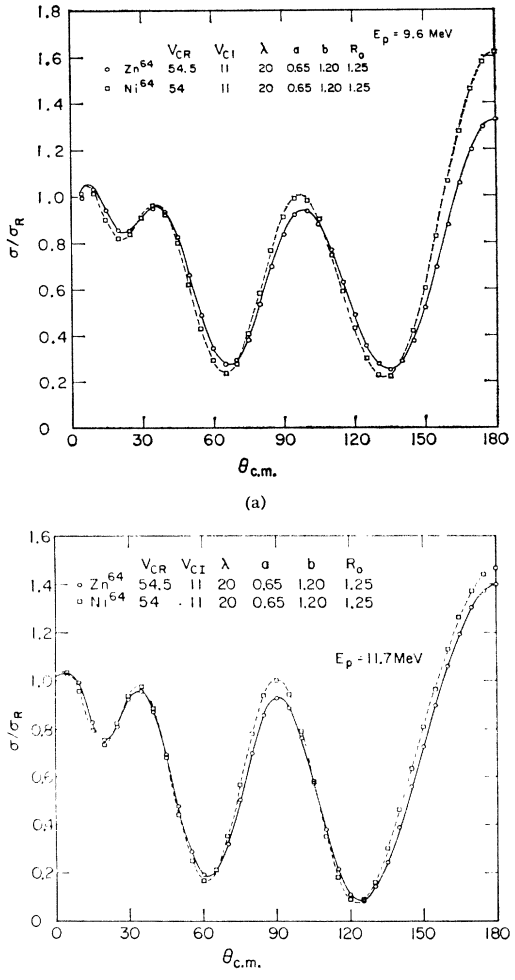

FIG. 5. Predictions of the optical model (without symmetry term). (a) E_p=9.6 MeV; (b) E_p=11.7 MeV.

Although the target thickness measurement had been checked repeatedly, it was recognized that the gravimetric technique gave an average thickness over the whole foil. Therefore, it was decided to survey the entire foil area with an instrument[44] designed to measure thickness variations by measuring the energy loss of penetrating Cm^{242} α particles. It was found that the foil was rather nonuniform and one side of the foil was considerably thinner than the center portion. A comparison with a very uniform, accurately weighed Cu foil showed that the portion of the Zn^{64} foil which was traversed by the beam was 10.0% thicker than the average thickness of the entire foil. Therefore all our measurements were high by this amount.

The correction has been applied to the data of Tables I and II and Figs. 3 and 4. The shift in phase of the oscillations for the two isobars is clearly discernible.

[40] J. Benveniste, A. C. Mitchell, and C. B. Fulmer, University of California Radiation Laboratory Report UCRL-6930, 1962 (unpublished).
[41] B. L. Cohen and R. V. Neidigh, Phys. Rev. **93**, 282 (1954).
[42] I. E. Dayton and G. Schrank, Phys. Rev. **101**, 1358 (1956).
[43] N. M. Hintz, Phys. Rev. **106**, 1201 (1957).
[44] J. Benveniste, A. Mitchell, C. Shrader, and J. Zenger, Rev. Sci. Instr. **32**, 927 (1961).

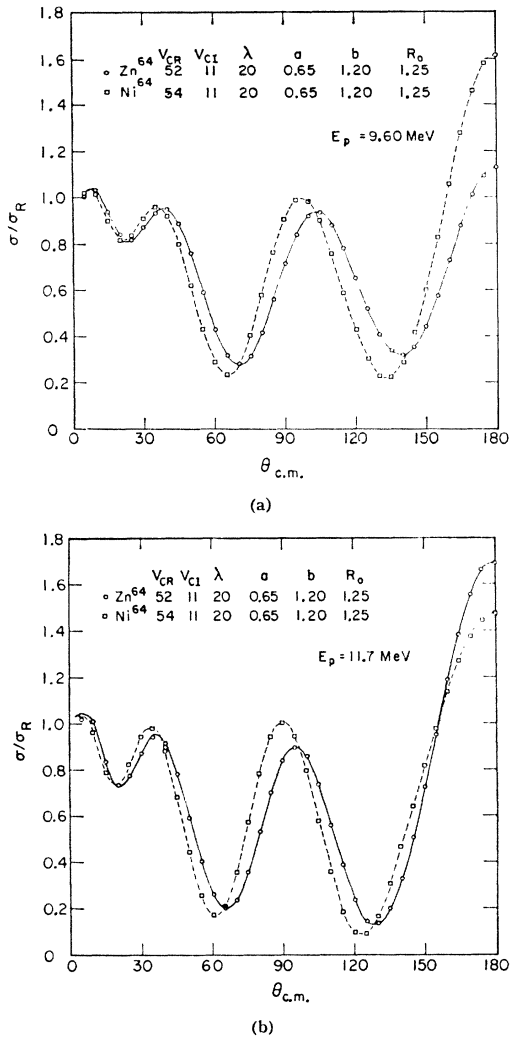

FIG. 6. Predictions of the optical model (with symmetry term). (a) E_p=9.6 MeV; (b) E_p=11.7 MeV.

A number of observations of this sort have been made with pairs of isotopes. For the most part, these have shown a shift which was larger than could be explained by the premise that the radius varies as $A^{1/3}$. Although this shift could equally well be understood in terms of an unexpected small departure of the radius from the $A^{1/3}$ law, this possibility was rejected in the case of the Cu-isotope observations[33] mainly on the strength of the lack of success of Beurtey *et al.*[26] in explaining their observations entirely in terms of a change of radius. Since then, however, corroborative evidence has been obtained for the correctness of this assumption.

Anderson and Wong,[35] in their study of neutron spectra from (p,n) reactions in medium-weight elements, have discovered transitions to states which are isobaric counterparts of the ground state of the bombarded nucleus. The final state is formed when the incoming proton knocks out a neutron, say from the $f_{7/2}$ shell, and itself enters the $f_{7/2}$ shell. Invoking the concept of charge independence of nuclear forces, the Q of the reaction should equal just the Coulomb energy of the last proton. Since the Coulomb energy is a function of the nuclear radius, it is clear that a measure of the excitation energy of the isobaric state is a measure of the nuclear radius. In their observations on Cu^{63} and Cu^{65}, Anderson and Wong found a difference in the excitation energies of 100±20 keV, the same difference one expects if the radius is governed by the $A^{1/3}$ law. In view of this success it is with considerably more confidence that we maintain our assumption that the nuclear radius is proportional to $A^{1/3}$.

The prediction of the optical model in its present form is shown in Figs. 5(a) and (b). The nuclear potential is given by

$$V=V_{CR}\rho(r)+iV_{CI}q(r)+\lambda\frac{1}{2M_p^2c^2}\left(\frac{1}{r}\frac{d}{dr}\rho(r)\right)\boldsymbol{\sigma}\cdot\mathbf{l},$$

$$\rho(r)=\frac{1}{1+e^{(r-R_0)/a}},\quad q(r)=e^{-[(r-R_0)/b]^2},\quad R_0=r_0A^{1/3},$$

where V_{CR} is the depth of the central, real potential; V_{CI} is the depth of the central, imaginary potential; λ fixes the magnitude of the spin-orbit potential; and a is the falloff parameter, and b is the width of the imaginary potential.

This is the form which has been found to be so successful in fitting a large gamut of elements over a considerable range of energies. The real potential V_{CR} is taken to be independent of A for a given energy; however, for protons this depth is increased by the value of the Coulomb potential at the nuclear surface—something close to $Z/A^{1/3}$. This is why V_{CR} differs by 0.5 MeV for Ni^{64} and Zn^{64} in Figs. 5(a) and (b).

It is clear that this form predicts an extremely small shift for the two isobars, considerably less than the magnitude of that observed. It might be suspected that the observed shift is being caused by other effects. For example, it can be shown that a compound elastic contribution would tend to shift minima to the left, and maxima to the right. However, since the (p,n) threshold is higher in Zn^{64}, we expect more compound elastic scattering for Zn^{64} and a consequent shift in the wrong direction. Or, one might consider effects due to nuclear deformation. The fact that the 2+ level of Zn^{64} is 0.36 MeV lower than the 2+ level of Ni^{64} indicates that Zn^{64} may be less spherical than Ni^{64}. In reference 38 elastic-scattering data from highly deformed nuclei are compared with data from spherical nuclei. Those data show that highly deformed nuclei do not produce appreciable shifts in angle of the diffraction pattern, but rather a damping of the amplitude of the oscillations of the σ/σ_R curves at large angles. To achieve this effect it is only necessary to increase the depth of the imaginary part of the nuclear potential.[23]

[45] J. D. Anderson, C. Wong, and J. W. McClure, Phys. Rev. **126**, 2170 (1962).

The required shift is obtained, however, if we invoke the suggestion that the real potential also depends on a symmetry energy term. Thus, V_{CR} might be described as

$$V_{CR}=V_0+Z/A^{1/3}+C(N-Z)/A,$$

where V_0 is the term which is independent of A, $Z/A^{1/3}$ is the Coulomb energy correction to the well, and $C(N-Z)/A$ is the symmetry energy.

For the two isobars under consideration here,

$$V_{CR}(\mathrm{Ni}^{64})=V_0+7+\tfrac{1}{8}C,$$
$$V_{CR}(\mathrm{Zn}^{64})=V_0+7.5+\tfrac{1}{16}C.$$

Therefore,

$$\Delta V_{CR}=\tfrac{1}{16}C-0.5.$$

Figure 6 shows the effect of introducing the symmetry energy term. No extensive search was made to find the optical-model parameters which would most closely fit the experimental data. Our major interest was to establish the fact of the shift and to explore the role of the symmetry energy term in the central, real potential.

By trial, we find that the optical-model calculations yield approximately the observed shift when $\Delta V_{CR}=2$ MeV. This yields $C=40$ MeV, a number which is in reasonable agreement with those found from other observations.

The (p,n) thresholds for Ni^{64} and Zn^{64} are 2.5 and 7.8 MeV, respectively, therefore one might expect compound-nucleus elastic scattering to contribute to the Zn^{64} data but not to the Ni^{64} data. In fact, evidence for this may be gathered from a comparison of the σ/σ_R plots. The 9.6-MeV plot shows a reasonably uniform displacement of one curve relative to the other up to the maxima near 100 deg; beyond this the displacement is larger for the decreasing part of the curves and disappears for the increasing portion of the curves beyond 140 deg. This difference is not observed in the 11.7-MeV σ/σ_R plots; the displacement of the two curves relative to each other is about the same throughout the angular distribution. This is consistent with a compound-nucleus elastic scattering contribution that diminishes as the incident proton energy is increased to a few MeV above the (p,n) threshold. The effect should be more noticeable at large angles where the absolute shape elastic scattering is small.

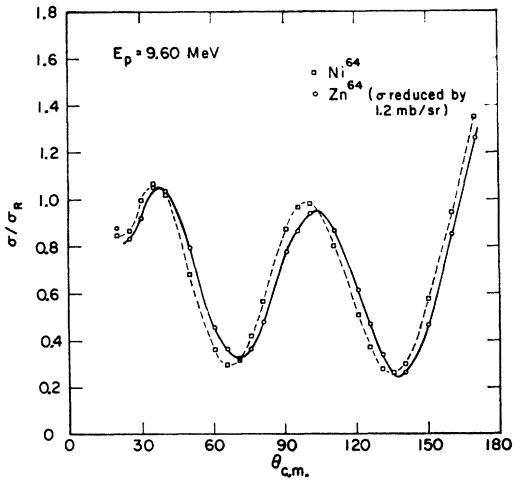

FIG. 7. 9.6-MeV σ/σ_R with compound-nucleus correction.

An estimate of the compund-nucleus elastic scattering was made as follows. Except near the maxima and minima (where the curves cross) the σ/σ_R plots for the 11.7-MeV data differ by approximately 0.1. This difference is observed in the 9.6-MeV plots up to about 95 deg. Beyond 140 deg the difference disappears. It is then assumed that compound-nucleus elastic-scattering contributes approximately 10% to the measured cross section at 150°, 160°, and 170°. The average value thus obtained is 1.2 mb/sr or a total of about 15 mb for the compound elastic scattering cross section for 9.6-MeV protons on Zn^{64}. This estimate is probably good to within a factor of 2.

For comparison Fig. 7 shows σ/σ_R plots of the 9.6 MeV data for which the measured cross sections of Zn^{64} have been reduced by 1.2 mb/sr.

ACKNOWLEDGMENTS

The authors are pleased to express their gratitude to Dr. E. H. Schwarcz for optical model calculations illustrating effects due to the presence and absence of the symmetry energy term, and to Professor J. S. Nodvik for conversations which helped place in perspective the state of development of the optical model.

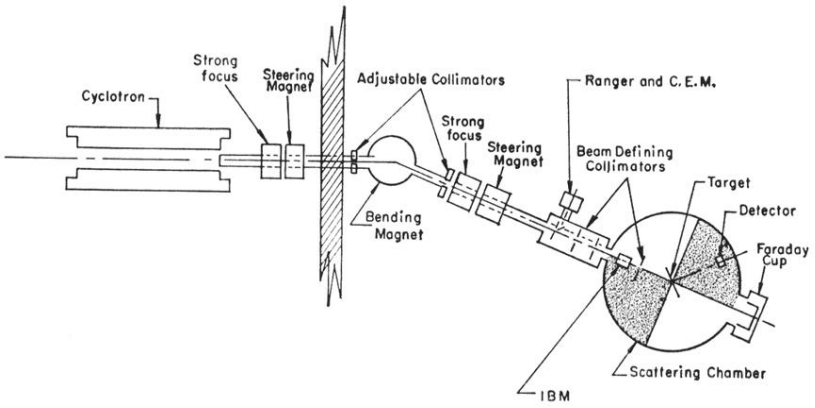

FIG. 1. Scattering geometry. The shaded sections of the scattering chamber indicate the regions in which observations were made.